Ti/Au Ultrathin Films For TES Application

Ti/Au Ultrathin Films For TES Application

Eugenio Monticone, Micaela Castellino, Roberto Rocci, Mauro Rajteri

***Abstract*—Transition-Edge Sensors (TESs) are versatile superconducting microcalorimeters used as single photon detectors in a large range of electromagnetic wavelength, from X-rays to near-infrared. Among the many materials investigated in literature, Ti/Au is one of the most widely used bilayer to fabricate TES thanks to simple deposition process, long term stability material and protection against oxidation of Ti film by Au over layer. Moreover, the critical temperature of Ti/Au can be tuned by trimming the thickness of Ti and Au films. For low energy photon detection, the Ti/Au superconducting layer performs simultaneously as absorber and thermometer. This implies that a TES thickness reduction helps to significantly reduce the thermal capacitance, which has a direct impact on the detector energy resolution. In this paper we present a study of the superconducting properties of Ti/Au films, grown in UHV by thermal evaporation as a function of Ti thickness. The chemical state of Ti and Ti/Au were analyzed by X-ray photoelectron spectroscopy, to evaluate the protective effect of Au film. The film morphology, structure and optical properties were investigated by ellipsometry. The critical temperature showed a marked trend on film thickness and was strongly affected by Au cover layer. Ti film of only 12 nm thick covered with 10 nm Au film showed a remarkable critical temperature of about 300 mK.**

***Index Terms*—Transition-edge sensors, XPS, Ellipsometry, UHV deposition.**

I. Introduction

TRANSITION-EDGE Sensors (TESs) are versatile superconducting microcalorimeters used as single photon detectors in a large range of the electromagnetic spectrum, from X-rays to near-infrared [1], [2]. Among the many materials investigated in literature, Ti is one of the most used both as single layer [3]–[6] or coupled to other high conductive metals like Ti/Au [7], Ti/Al [8], Ti/Pd [9]. Bilayers have the great advantage of opening the possibility to tune the transition temperature by trimming the thickness of the normal metal film. In this paper we concentrate our investigation on the widely used Ti/Au bilayer. For detection of low energy visible photons, the Ti/Au bilayer performs simultaneously as absorber and thermometer. This implies that a TES thickness reduction helps to significantly reduce the thermal capacitance, which has a direct impact on the detector energy resolution. A reduced thickness also gives practical advantages in fabrication of detectors with small dimensions as nanowires and nanobridges where nanolitography is employed [10], [11]. In this paper we present a study of superconducting properties of Ti/Au films as a function of Ti thickness grown in UHV by thermal evaporation. The chemical state of Ti and Ti/Au were analyzed by X-ray photoelectron spectroscopy, to evaluate the protective effect of Au film. The film morphology, structure and optical properties were investigated by ellipsometry.

Manuscript received November 30, 2020; revised February 17, 2021; accepted March 18, 2021. Date of publication March 31, 2021; date of current version May 17, 2021. *(Corresponding author: Eugenio Monticone.)*

Eugenio Monticone, Roberto Rocci, and Mauro Rajteri are with the Istituto Nazionale di Ricerca Metrologica, 10135 Torino, Italia (e-mail: e.monticone@inrim.it).

Micaela Castellino is with the Department of Applied Science and Technology, Politecnico di Torino, Torino 10129, Italy (e-mail: micaela.castellino@polito.it).

Color versions of one or more figures in this article are available at https://doi.org/10.1109/TASC.2021.3069903.

II. Experimental Details

Ti/Au bilayers were fabricated by thermal evaporation of Ti films and Au films on 500 nm silicon nitride on silicon substrate in UHV at a base pressure $<5 \times 10^{-9}$ mbar. Before introducing the substrate in the deposition system, from load-lock, its surface was ion milled to remove the contaminants. Films were deposited after the recovery time of the base pressure. During deposition of Ti the pressure was close to 5×10^{-8} mbar, lowering below 10^{-8} mbar during Au deposition. The deposition rate for Ti and Au were 0.3 nm/s and 0.02 nm/s, respectively. Waiting time between the end of Ti deposition and the start of the Au deposition was less than 10 s in order to reduce Ti oxidation. [12]. Because interdiffusion between Au and Ti has been observed at relatively low temperature [13] the substrate temperature was monitored during deposition. It was observed a maximum temperature increasing of about thirty degree above room temperature, a value at which the interdiffusion should be negligible [13].

Film thicknesses were monitored by using a quartz microbalance calibrated with samples of different thickness measured by AFM and optical profilometer.

Thickness and optical properties of thin films can be obtained with non-invasive method applying ellipsometry, an optical technique based on the measurement of elliptically polarized light. Measured ellipsometric quantities are expressed as psi (ψ) and delta (Δ), values related to the optical properties of the material, through the ratio of the Fresnel reflection coefficients r_p and r_s (polarization p and s, respectively) of the sample, by the relationship

$$\rho = r_p / r_s = \tan(\psi)\, \mathrm{e}^{\mathrm{i}\Delta}$$

where ρ is the complex reflectance ratio. In polar coordinates $\tan(\psi)$ is the magnitude of the ratio of the p to s amplitude reflection coefficients of the material and Δ is the phase difference between the p and s reflection coefficients. The phase information Δ gives the measurement technique sensitivity, which exceeds that of intensity reflectance measurements. Spectroscopic ellipsometric data for each film were collected with a variable-angle spectroscopic ellipsometer (VASE). Measurements were taken

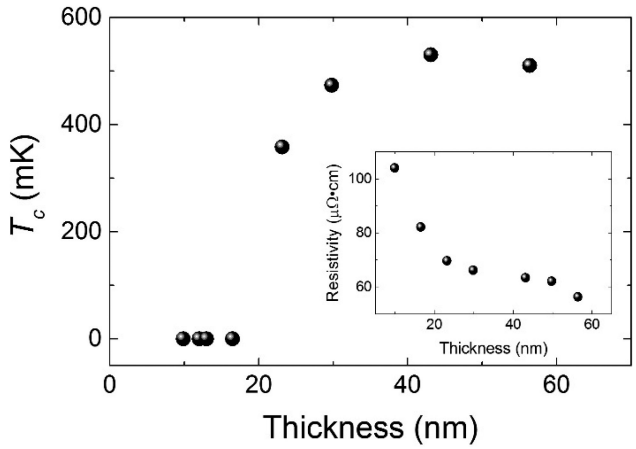

Fig. 1. Critical temperature T_c vs thickness of Ti films. In the inset is shown the film resistivity at room temperature.

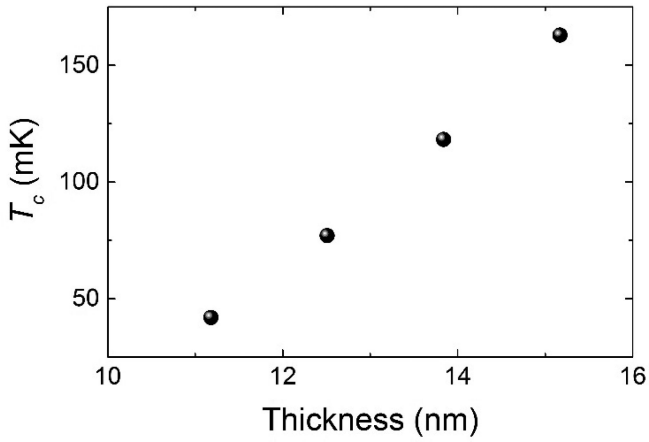

Fig. 2. Critical temperature T_c vs thickness of Ti films covered with 27 nm of Au.

from 350 nm to 1700 nm at two angles, typically 70° and 76°, at 20 nm steps.

A PHI 5000 Versaprobe Scanning X-ray Photoelectron Spectrometer (monochromatic Al K-α Xray source with 1486.6 eV energy) was used to investigate the surface chemical composition.

A spot size of 100 μm was used in order to collect the photoelectron signal for both the high resolution (HR) and the survey spectra. All samples were analyzed with a combined electron and Ar ion gun neutralizer system in order to reduce the charging effect during the measurements. All core-level peak energies were referred to Au($4f_{7/2}$) peak at 84.0 eV and the background contribution in HR scans was subtracted by means of a Shirley function. Spectra were analyzed using Multipak 9.6 dedicated software. Depth profile, by means of an Ar+ flux at 2 kV accelerating voltage, has been performed in an alternate mode with sputtering cycles of 6 s each, in order to reduce the Au thin film to get the signal from Ti(2p) underneath. The Ti oxide thin film thickness (l) has been evaluated by [14]:

$$l \; = \; -\lambda_{Ti,ox} \cdot \cos\varphi \cdot ln\,(R/R + R^*)$$

where $\lambda_{Ti,ox}$ is the inelastic mean free path (IMFP) of photoelectrons in Ti oxide (2.35 nm), $\lambda_{Ti,m}$ is the IMFP in Ti metal film (1.74 nm). φ is the photoelectron take-off angle (0.79 rad), $R \; = I_{Ti,m}/I_{Ti,ox}$ and $R^* = \lambda_{Ti,m} \cdot C_{Ti,m}/\lambda_{Ti,ox} \; \cdot C_{Ti,ox}$, where $I_{Ti,m}$ is the peak intensity related to Ti metal state, while $I_{Ti,ox}$ is the peak intensity related to Ti oxide. $C_{Ti,m}$ is Ti metal concentration (94.78 kmol/m^3) and $C_{Ti,ox}$ is Ti oxide concentration (53.57 kmol/m^3).

III. Results

A. Superconducting Properties

The critical temperature for superconductors is the temperature at which the electrical resistivity drops to zero. It is extracted from the experimental data at the midpoint of the resistive transition. The uncertainty in the T_c measurement is dominated by the calibration uncertainty of our thermometer that is 5 mK

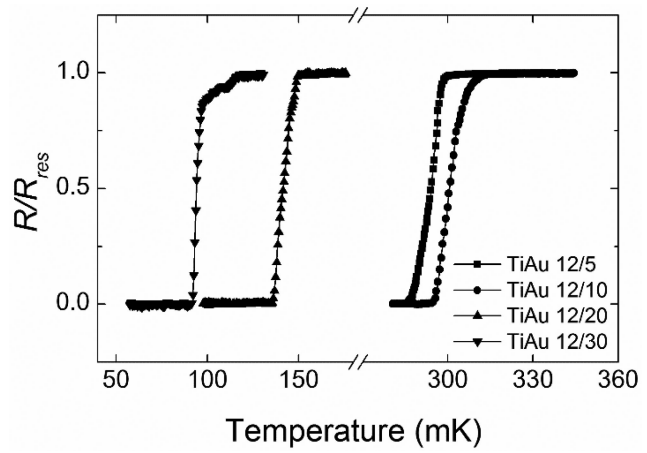

Fig. 3. Resistance, normalized to normal-state resistance R_{res}, vs temperature for Ti/Au films with increasing Au thickness as reported in the legend in nm.

under 150 mK and 10 mK above 150 mK. In Fig. 1 is shown the critical temperature T_c of Ti films as a function of the thickness and in the inset the resistivity at room temperature is reported. A film only 30 nm thick has a T_c of 500 mK, close to bulk value, that confirms the good film quality, but 18 nm thick or thinner films do not show T_c within the base temperature of our refrigerator, about 30 mK. When Ti film is exposed to air, in addition to the formation of few nm of Ti oxide, there is an extensive penetration of oxygen into the film of the order of tens of nanometers [15], which affects film superconducting properties. A frequent reported solution to avoid air oxidation is to cover Ti films with noble metals, in particular Au films [16]. In Fig. 2 critical temperatures of very thin Ti films covered with 27 nm of gold are plotted. Thanks to Au protection, a film of about 12 nm has a transition temperature of 80 mK. In Fig. 3 are reported the transition curves of TiAu films, where the thickness of Ti is fixed to 12 nm and Au thicknesses range from 5 to 30 nm. T_c saturates for thinner Au films indicating that the value of T_c for such Ti films is close to 300 mK. By increasing Au thickness we observe a strong reduction of T_c to

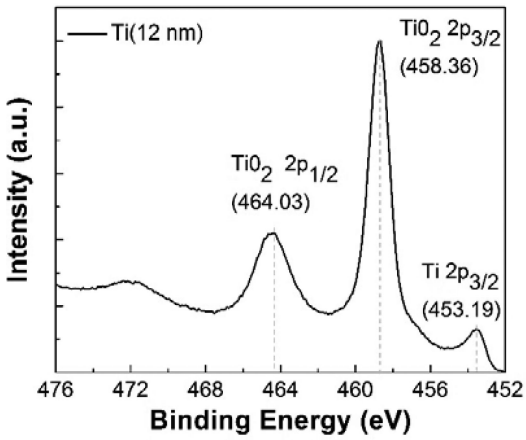

Fig. 4. XPS spectrum of Ti film showing the main peaks attribute to TiO_2 and Ti.

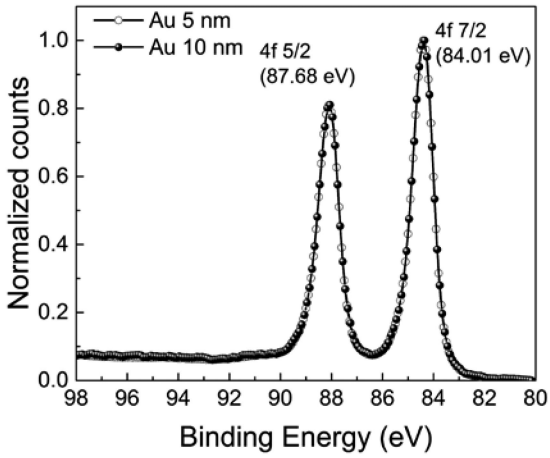

Fig. 6. XPS spectra of TiAu films, for two different Au thicknesses as reported in the legend, with two peaks attributed to metal Au.

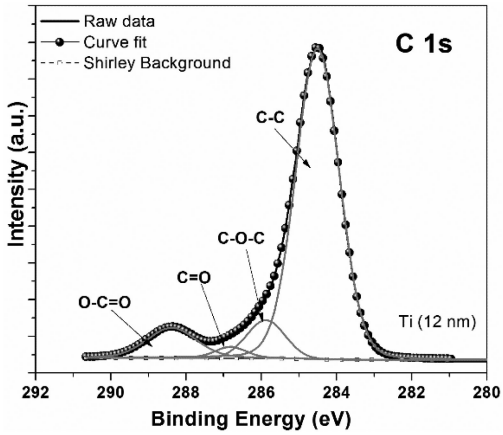

Fig. 5. XPS spectrum of Ti 12 nm film showing the C 1s HR region, together with its deconvolution procedure, used to identified chemical shifts due to ambient contamination [17].

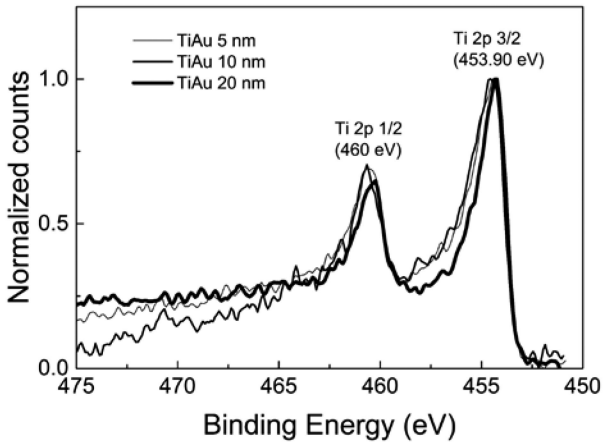

Fig. 7. XPS spectra of TiAu bilayer after ion-sputtering of Au film. Only Ti peak (Ti 2p1/2) and satellite (Ti 2p3/2) were observed.

witness an effective proximity effect; moreover the increase in Au thickness induces also a reduction of the transition width due to a better temperature uniformity favored by the Au high diffusivity.

B. XPS Analysis

The same samples characterized from the superconductive point of view have also been characterized with XPS analysis to obtain information on chemical state and composition of Ti and TiAu films. Spectra of Ti film 12 nm thick is show in Fig. 4, where it is possible to recognize two main peaks related to stoichiometric TiO_2 and a smaller peak at binding energy of 453.19 eV typical of metallic Ti. Thickness of Ti oxide has been evaluated from relation in [17] to be 3.6 ± 0.2 nm in agreement with neutron reflectometry technique [18]. From XPS spectra has been estimated a high concentration of oxygen (50%) and carbon (30%) due to ambient exposure (see fig. 5) [17], that is the likely reason for the T_c suppression. XPS analysis spectra of TiAu film is illustrated in Fig. 6, with peaks resulting from Au 4f $_{5/2}$ and 4f $_{7/2}$ electrons. No other peaks were visible in case of thicker Au film (20 and 10 nm), while a small peak of Ti was observed for thinner Au film (5 nm). With the purpose to analyze the TiAu interface, the Au films were etched by sputtering at a constant rate for 6 s followed by analysis in order to detect Ti oxidation accurately. After a non-complete sputtering of Au films Ti 2p doublet was detected, which has to be ascribed to Ti(0), but no peaks of Ti oxide were observed (Fig. 7).

In fig. 8 we show also survey spectrum together with C 1s HR region (see inset) for sample TiAu 20 nm (after Ar+ sputtering), to underline that adventitious C was not detected in the Ti/Au interface region, due to the absence of a layer of contamination during Ti/Au deposition (same results for samples 10 nm and 5 nm, not reported).

XPS data show that few nm of Au effectively protect Ti from oxidation.

C. Ellipsometry

To estimate parameters as thickness, morphology and optical properties from the measured ellipsometric data ψ and Δ, we need a model for the refractive index of each sample layer.

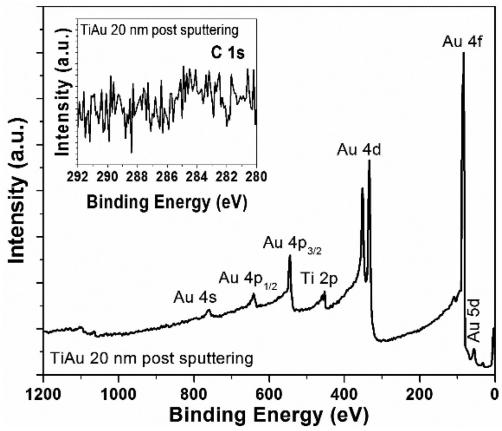

Fig. 8. XPS survey spectrum of TiAu 20 nm post Ar+ sputtering, showing only peaks related to Ti and Au. In inset C 1s region has been reported to confirm the absence of adventitious C in Ti/Au interface.

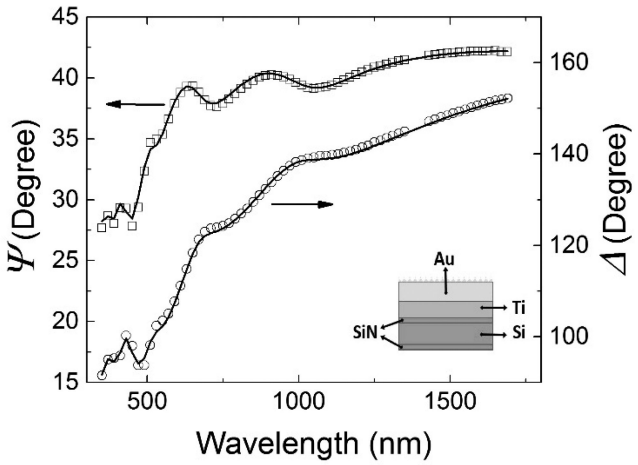

Fig. 9. Psi-Delta vs wavelength experimental data (open symbol) of TiAu sample with 20 nm thick Au film fitted (solid line) using the model described in the text. In the inset is shown the layer model of the sample.

For our bilayer films, after the information obtained from the XPS technique, we choose the structure reported in the inset of Fig. 9. Si substrate has modelled using a tabulated set of data for semiconductor grade silicon single crystal [19], while for SiN amorphous layer the analytical model used is a modified Tauc Lorentz function [20]. For Ti films the optical constants found in literature did not provide good fit; we built a material model based on three Lorentz oscillators [21] to get a good match with the experimental data, while for Au tabulated data are a good solution [22]. Au roughness is modelled by an effective medium approximation (EMA) layer composed of 50% bulk material and 50% void. The thickness of this layer is correlated to rms roughness of film surface. The roughness of Ti/Au films was obtained by AFM on a scanned area of 1 μm x 1 μm. The rms roughness value are shown in Table I.

The fit parameters are the complex refractive indexes (n, the real component, and k, the imaginary component) and the thicknesses of every layer, for each sample. To reduce the number of fit parameters, we used the multiple sample analysis (MSA)

TABLE I
COMPARISON AMONG THE FILM THICKNESSES MEASURED WITH THE MICROBALANCE AND OBTAINED FROM THE FIT OF THE ELLIPSOMETRIC DATA

Quartz microbalance	Ellipsometry		AFM
Ti/Au (nm)	Au (nm)	Ti (nm)	Roughness (nm)
12/5	4.9±0.1	13.1±0.1	0.6±0.1
12/10	9.2±0.1	13.2±0.1	0.7±0.1
12/20	21.9±0.2	13.2±0.4	1.0±0.1

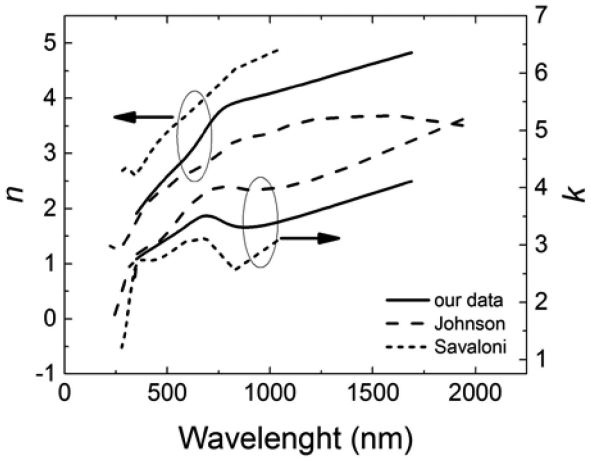

Fig. 10. Refractive index n and extinction coefficient k of Ti film evaluated by Lorentz oscillators with parameters obtained by fitting the TiAu samples. The optical constant of Ti films grown in ultra high vacuum (Savaloni) and high vacuum (Johnson) are shown, for comparison purpose.

by assuming the same optical functions for all samples and by varying only the thickness from sample to sample. The minimum value found for MSE (mean-squared-error) of the fit was 7.8. In Fig. 9 are shown experimental data ψ and Δ (open symbols) with the best fit (solid curve). The corresponding behaviour of n and k as a function of wavelength for Ti (–) are reported in Fig. 10. For comparison are also reported the optical constant of Ti films grown in ultra high vacuum (Savaloni) [23] and high vacuum (Johnson) [24]. Thicknesses fit parameters are reported in Table I. Au and Ti thicknesses are in agreement with thicknesses measured by the quartz microbalance.

IV. CONCLUSION

The performances of superconducting detectors like TESs are strictly related to the heat capacity of the detector. A reduction of the film thicknesses can therefore allow to improve the detector energy resolution. This study highlight the possibility to obtain a very thin superconductive Ti layer of 12 nm if a protective gold layer is quickly deposited after the Ti film. XPS analysis indicated the absence of a Ti oxide layer between Ti and Au film; moreover, thickness were also confirmed by ellipsometric analysis and the optical refractive index of Ti obtained from the same fit procedure.

REFERENCES

[1] J. N. Ullom, and D. A. Bennett, "Review of superconducting transition-edge sensors for X-ray and gamma-ray spectroscopy," *Supercond. Sci. Technol.*, vol. 28, 2015, Art. no. 084003.

[2] L. Lolli, E. Taralli, C. Portesi, E. Monticone, and M. Rajteri, "High intrinsic energy resolution photon number resolving detectors," *Appl. Phys. Lett.*, vol. 103, 2013. Art. no. 041107.

[3] B. S. Karasik, A. V. Sergeev, and D. E. Prober, "Nanobolometers for THz photon detection," *IEEE Trans. Terahertz Sci. Technol.*, vol. 1, no. 1, pp. 97–111, Sep. 2011.

[4] D. Fukuda *et al.*, "Titanium-based transition-edge photon number resolving detector with 98% detection efficiency with index-matched small-gap fiber coupling," *Opt. Exp.*, vol. 19, pp. 870–875, 2011.

[5] Z. Wang *et al.*, "Electron-beam evaporated superconducting titanium thin films for antenna-coupled transition edge sensors," *IEEE Trans. Appl. Supercond.*, vol. 28, no. 4, Jun. 2018, Art. no. 2100204.

[6] W. Zhang *et al.*, "Development of titanium-based transition-edge single-photon detector," *IEEE Trans. Appl. Supercond.*, vol. 29, no. 5, Aug. 2019, Art. no. 2100505.

[7] K. Nagayoshi *et al.*, "Development of a Ti/Au TES microcalorimeter array as a backup sensor for the Athena/X-IFU instrument," *J. Low Temp. Phys.*, vol. 199, pp. 943–948, 2020.

[8] L. Lolli, E. Taralli, C. Portesi, M. Rajteri, and E. Monticone, "Aluminum–Titanium bilayer for near-infrared transition edge sensors," *Sensors*, vol. 16, 2016, Art. no. 953.

[9] E. Taralli, C. Portesi, R. Rocci, M. Rajteri, and E. Monticone, "Investigation of Ti/Pd bilayer for single photon detection," in *IEEE Trans. Appl. Supercond.*, vol. 19, no. 3, pp. 493–495, Jun. 2009.

[10] Z. M. Wang, J. S. Lehtinen, and K. Yu. Arutyunov, "Towards quantum phase slip based standard of electric current," *Appl. Phys. Lett.*, vol. 114, 2019, Art. no. 242601.

[11] C. Portesi, E. Taralli, L. Lolli, M. Rajteri, and E. Monticone, "Fabrication and characterization of fast TESs with small area for single photon counting," *IEEE Trans. Appl. Supercond.*, vol. 25, no. 3, Jun. 2015, Art. no. 220034.

[12] M. L. Ridder *et al.*, "Fabrication of low-noise TES arrays for the SAFARI instrument on SPICA," *J. Low Temp. Phys.*, vol. 184, pp. 60–65, 2016.

[13] N. J. van der Heijden *et al.*, "Diffusion behaviour in superconducting Ti/Au bilayers for SAFARI TES detectors," *J. Low Temp. Phys.*, vol. 176, pp. 370–375, 2014.

[14] K. E. Healy, and P. Ducheyne, "Oxidation kinetics of titanium thin films in model physiologic environments," *J. Colloid Interface Sci.*, vol. 150, no. 2, pp. 404–417, 1992.

[15] A. H. J. van den Berg, W. Lisowski, and M. Smithers, Fresenius, "SEM and AES depth profile studies of thin titanium and titanium oxide films covered by nanoscale evaporated au layers," *J. Anal. Chem.*, vol. 365, pp. 231–235, 1999.

[16] G. Fujii *et al.*, "Thin gold covered titanium transition edge sensor for optical measurement," *J. Low Temp. Phys.*, vol. 167, pp. 815–821, 2012.

[17] T. L. Barr, and S. Seal, "Nature of the use of adventitious carbon as a binding energy standard," *J. Vac. Sci. Technol. A*, vol. 13, pp. 1239–1246, 1995.

[18] V. A. Matveev *et al.*, "The study of the oxidation of thin Ti films by neutron reflectometry," *J. Phys.: Conf. Ser.*, vol. 340, 2012, Art. no. 012086.

[19] C. M. Herzinger, B. Johs, W. A. McGahan, J. A. Woollam, and W. Paulson, "Ellipsometric determination of optical constants for silicon and thermally grown silicon dioxide via a multi-sample, multi-wavelength, multi-angle investigation," *J. Appl. Phys.*, vol. 83, pp. 3323–3336, 1998.

[20] D. V. Likhachev, N. Malkova, and L. Poslavsky, "Modified tauc–Lorentz dispersion model leading to a more accurate representation of absorption features below the bandgap," *Thin Solid Films*, vol. 589, pp. 844–851, 2015.

[21] G. Droulers, A. Beaumont, J. Beauvais, and D. Drouin, "Spectroscopic ellipsometry on thin titanium oxide layers grown on titanium by plasma oxidation," *J. Vac. Sci. Technol. B*, vol. 29, no. 2, 2011, Art. no. 021010.

[22] J. A. Woollam Co., WVASE manual "Guide to using WVASE32," 2010.

[23] H. Savaloni, and H. Kangarloo," Influence of film thickness, substrate temperature and nano-structural changes on the optical properties of UHV deposited ti thin films," *J. Phys. D: Appl. Phys.*, vol. 40, pp. 203–214, 2006.

[24] P. B. Johnson, and R. W. Christy, "Optical constants of transition metals: Ti, V, Cr, Mn, Fe, Co, Ni, and Pd," *Phys. Rev. B.*, vol. 9, pp. 5056–5070, 1974.